Nephrin and podocin dissociate at the onset of proteinuria in experimental membranous nephropathy

TAKESHI NAKATSUE, HIROKO KOIKE, GI DONG HAN, KOICHI SUZUKI, NAOKO MIYAUCHI, HUAIPING YUAN, DAVID J. SALANT, FUMITAKE GEJYO, FUJIO SHIMIZU, and HIROSHI KAWACHI

Department of Cell Biology, Institute of Nephrology, Niigata University Graduate School of Medical and Dental Sciences, Niigata, Japan; Division of Clinical Nephrology and Rheumatology, Niigata University Graduate School of Medical and Dental Sciences, Niigata, Japan; and Renal Section and Department of Medicine, Evans Biomedical Research Center, Boston University Medical Center, Boston, Massachusetts

Nephrin and podocin dissociate at the onset of proteinuria in experimental membranous nephropathy.

Background. The slit diaphragm plays a critical role in maintaining the barrier function of the glomerular capillary wall. The pathogenic mechanism of proteinuria in membranous nephropathy remains uncertain. This study was undertaken to analyze the pathogenic role of slit diaphragm in proteinuria in experimental membranous nephropathy.

Methods. The expression and the localization of slit diaphragm–associated molecules (nephrin, podocin, and CD2AP) and other podocyte-associated molecules (podocalyxin and α_3 integrin) in passive and active Heymann nephritis were analyzed by immunofluorescence and Western blot analysis. The interaction of slit diaphragm–associated molecules was investigated by the dual-labeling immunofluorescence method. The mRNA expression of these molecules was also analyzed.

Results. Shifts in nephrin and podocin staining patterns, from linear to granular, were detected in the early stages of passive Heymann nephritis. These shifts were not parallel, and the dissociation of these molecules was detected by the dual-labeling immunofluorescence method in passive and active Heymann nephritis. Western blot analyses with sequentially solubilized materials indicated that the nephrin-rich fraction changed from being partly detergent-resistant to being predominantly detergent-soluble. This change did not occur with podocin. Nephrin excreted into urine was already detected in the early stages of passive Heymann nephritis. Decreased mRNA expression of nephrin and podocin was observed before the onset of proteinuria. By contrast, no extensive change in the expression of α_3 integrin was observed in this study.

Conclusion. Nephrin is dissociated from podocin and excreted into urine in the early stages of Heymann nephritis. The reduced expression of nephrin and podocin, along with their dissociation, may contribute to the development of proteinuria in Heymann nephritis.

Membranous nephropathy is characterized by subepithelial immune deposits and effacement of the podocyte foot processes. The primary clinical manifestation is proteinuria. Although podocyte injury and proteinuria are mediated in membranous nephropathy by the membrane attack complex of complement [1], the pathogenic mechanism of proteinuria in membranous nephropathy has not been clarified yet. Nephrin is identified as a product of *NPHS1* [2], and is considered to be a critical component of the epithelial slit diaphragm, maintaining the barrier function of the glomerular capillary wall [3]. Recently, some investigators reported that nephrin expression is decreased at the mRNA level and/or the protein level in membranous nephropathy [4–6]. However, another report showed that the expression of nephrin mRNA and protein was unchanged in patients with membranous nephropathy [7]. These discrepancies might stem from the differences in the quantitative methods used for analysis. It is also conceivable that the difference in the phase of the disease at which the materials were obtained may result in these contradictory results. Although an investigation of the kinetics of nephrin expression is necessary to clarify the etiologic significance of its decreased expression for the development of proteinuria in membranous nephropathy, there are restrictions on analyzing human biopsy material. Heymann nephritis in rats is widely used as an experimental model of idiopathic membranous nephropathy [8]. Heymann nephritis can be modeled in two major ways: the active type, induced by direct immunization with a rat kidney suspension of fraction 1A (Fx1A) of kidney lysate [9], and the passive type, induced by a passive injection of anti-Fx1A antibody produced in other animal species, such as rabbits or sheep [10, 11]. Although it has been pointed out that some pathogenic mechanisms differ between these two types of model [12], both are accepted as models of human idiopathic membranous nephropathy. Recently, our group reported that nephrin expression decreased in the

early stages of passive Heymann nephritis [13, 14], which suggests that the decreased expression of nephrin was involved in the development of proteinuria in membranous nephropathy. In the previous report, our group showed that nephrin dissociated from actin in this disease. These observations suggest that the dissociation of nephrin from actin may underlie the loss of the podocyte barrier function in membranous nephropathy [13]. However, what disrupts the nephrin-actin interaction and how nephrin-actin dissociation results in podocyte dysfunction remains unresolved.

Following nephrin, several other slit diaphragm–associated molecules, such as podocin, CD2AP and NEPH1, were identified [15–18]. Although the expression of nephrin and CD2AP has been reported in passive Heymann nephritis [13], no studies on the expression of podocin in membranous nephropathy have been reported. In active Heymann nephritis, slit diaphragm–associated molecules have not yet been analyzed. Recently, the interaction of nephrin with other slit diaphragm–associated molecules was analyzed by pull-down assay, using cultured cells expressing these molecules [19–22]. These studies showed that cytoplasmic segments of nephrin bind to the C-terminal site of podocin [19, 20] and CD2AP [23, 24]. However, the nature of the interactions in vivo between slit diaphragm–associated molecules has remained uncertain, despite some reported studies on their expression [25–27].

In this study, the expressions of nephrin, podocin, and CD2AP in both passive and active Heymann nephritis were analyzed, as well as urinary nephrin and podocin excretion in passive Heymann nephritis. Then, the interaction between these slit diaphragm–associated molecules in the models was examined. Immunohistochemical and polymerase chain reaction (PCR) studies clearly showed that not only nephrin but also podocin expression decreases during the early stages of the disease, prior to the observation of proteinuria. We detected urinary nephrin on day 7 of passive Heymann nephritis, when abnormal proteinuria had not yet been detected. Dual-labeling immunohistochemistry and Western blot analysis with sequentially solubilized materials of glomerular lysate showed that nephrin dissociates from podocin in the proteinuric state. These findings suggest that the alteration in slit diaphragm component interaction, as well as the decrease in their expression, may be the mechanism of proteinuria in membranous nephropathy.

METHODS

Animals

Specific pathogen-free female Wistar, male Sprague-Dawley, and male Lewis rats were purchased from Charles River Japan (Atsugi, Japan). All animal experiments conformed to the National Institute of Health Guide for the Care and Use of Laboratory Animals.

Preparation of Fx1A and anti-Fx1A antibodies

Fx1A was prepared in accordance with the method of Edgington, Glassock, and Dixon [9], Edginton et al [28], and de Heer, Daha, and van Es [29], with minor modifications. The rabbits were immunized with Fx1A four times, and bled 2 weeks after the last immunization. The serum obtained was incubated for 30 minutes at 56°C, so that the complements could be inactivated and adsorbed into the rat red blood cells. Sheep anti-Fx1A was prepared as described in another report [30].

Experimental protocol

Experiment 1: Studies on passive Heymann nephritis induced by rabbit anti-Fx1A antibody (passive Heymann nephritis rabbit). Passive Heymann nephritis was induced in 16 female Wistar rats by a single intravenous injection of 2 mL of rabbit anti-Fx1A (passive Heymann nephritis rabbit). Five rats each were sacrificed on days 1 and 7, and three rats each on days 14 and 42. As a control group, five age-matched normal rats were sacrificed. Half of their left kidneys was cut into portions and used for light microscopy, electron microscopy, and immunofluorescence. The deposition of injected rabbit IgG, rat IgG, and rat C3 was analyzed with fluorescein isothiocyanate (FITC)-conjugated antirabbit immunoglobulins (Dako, Glostrup, Denmark), FITC-conjugated antirat immunoglobulins (Dako) and FITC-conjugated antirat C3 (Cappel, Aurora, OH, USA), respectively. The expression of nephrin, podocalyxin, and α_3 integrin was investigated by immunofluorescence staining with murine monoclonal antinephrin antibody 5-1-6 [31–33], murine monoclonal antipodocalyxin antibody donated by Dr. M. Hara (Yoshida Hospital, Niigata, Japan) [34], and murine monoclonal antibody against α_3 integrin purchased from Santa Cruz Biotechnology, Inc. (Santa Cruz, CA, USA). The α_3 subunit of integrin binds only to the β_1 subunit of integrin, although the β_1 subunit binds to various subunits of integrin. Therefore, in this study, we used the anti-α_3 subunit of integrin to detect the $\alpha_3\beta_1$ integrin, which is reported to connect the basal surface of the podocyte to the glomerular basement membrane [35–37]. In order to evaluate the staining patterns of nephrin, we scored them in accordance with the method described by Macconi et al [38]. A score was assigned to each individual glomerulus in the tissue section. The scores 0, 0.5, and 1.0 were used, respectively, for continuous distribution along the glomerular capillary wall, heterogeneous distribution along the glomerular membrane (with variable staining intensity from one region to another within the same glomerulus), and markedly discontinuous distribution. The final score per section was then calculated as

the weighted mean: score = $(N_1 \times 0 + N_2 \times 0.5 + N_3 \times 1)/(N_1 + N_2 + N_3)$, where N_i (i = 1 to 3) is the number of glomeruli in each category. The scores were assigned blindly. On average, more than 80 glomeruli per section were evaluated.

Twenty-four–hour urine samples were collected just before (day 0) and on days 3, 5, 7, 11, 14, 21, 28, 35, and 42 after anti-Fx1A antibody injection. The amount of urinary protein excretion was measured by the Bradford method (Bio-Rad, Oakland, CA, USA). Urine samples from rats on days 0 and 7 of passive Heymann nepritis rabbit were used for Western blot analysis. Fifteen microliters of urine per lane were subjected to sodium dodecyl sulfate-polyacrylamide gel electrophoresis (SDS-PAGE) with 7.5% or 10% acrylamide gel, in accordance with the method of Laemmli [39], and transferred to polyvinylidine difluoride (PVDF) membrane strips. These strips were then exposed to rabbit antirat nephrin antibody [32] or rabbit antirat podocin N-terminus antibody [40] and incubated with alkaline phosphatase–conjugated antirabbit immunoglobulins (Bio Source International, Tago Immunologicals, Camarillo, CA, USA). The reaction was developed with an alkaline phosphatase chromogen kit (5-bromo-4-chloro-3-indolil phosphate p-toluidine salt/nitro blue tetrazolium) (Biomedica, Foster City, CA, USA).

Glomerular RNA was prepared from the remaining kidney tissues pooled from five rats at each time point. Glomerular mRNA expressions of nephrin, podocin, and CD2AP in the early phase (days 0, 1, and 7) were analyzed by the real-time reverse transcription (RT)-PCR method.

Experiment 2: Studies on passive Heymann nephritis induced by sheep anti-Fx1A antibody (passive Heymann nephritis sheep). Passive Heymann nephritis was induced in three male Sprague-Dawley rats by two intravenous injections of sheep anti-Fx1A, 0.25 mL and 0.5 mL, on successive days (passive Heymann nephritis sheep). Some antibodies used for detecting the slit diaphragm components are rabbit antibodies and are not available in passive Heymann nephritis rabbit, so we prepared passive Heymann nephritis sheep. The rats were sacrificed on day 7 after the first injection. As a control group, three age-matched normal rats were sacrificed. Twenty-four–hour urine samples were collected just before injection (day 0), on day 4, and just before sacrifice. Small pieces of their kidney tissues were snap-frozen and used for immunofluorescence. The stainings of nephrin, podocin, CD2AP, podocalyxin, and α_3 integrin were investigated. Two antibodies each for nephrin, podocin, and CD2AP were prepared. For nephrin, murine monoclonal ant-nephrin antibody 5-1-6 (which recognizes the extracellular site of nephrin) [31–33] and rabbit antinephrin antibody (which recognizes the intracellular site of nephrin) [32] were used. For podocin, antibody against the N-terminus of podocin was prepared as pre-
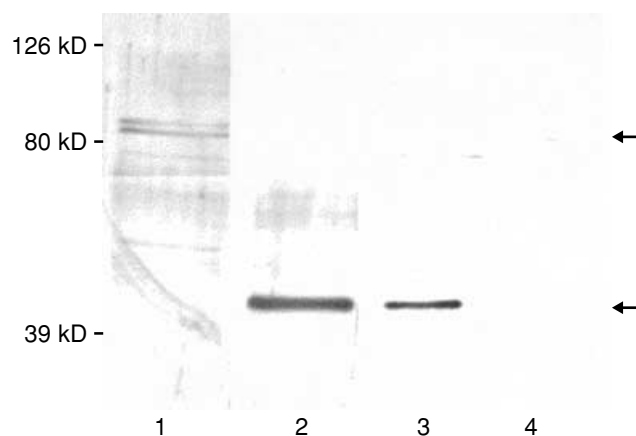
Fig. 1. Western blot analysis of the solubilized glomerular proteins with antipodocin and anti-CD2AP antibodies. Normal rat glomeruli were solubilized with sodium dodecyl sulfate-polyacrylamide gel electrophoresis (SDS-PAGE) sample buffer. The solubilized glomeruli were loaded onto a 10% polyacrylamide gel, electrophoresed, and transferred to a polyvinylidine difluoride (PVDF) membrane. The stripes were stained with alkaline phosphatase–conjugated antirabbit immunoglobulins after exposure with anti-CD2AP antibody (NI21-25) (lane 1), antipodocin antibody against the N-terminus of podocin (lane 2), antipodocin antibody against the C-terminus of podocin (lane 3), or preimmune rabbit serum (lane 4). Bands of approximately 80 kD were detected by anti-CD2AP antibody (NI21-25) (lane 1). A band of approximately 42 kD was detected by antipodocin antibodies (lanes 2 and 3). No bands were detected by the preimmune rabbit serum (lane 4).

viously described [40]. Antibody against the C-terminus of podocin was prepared in rabbits immunized with a peptide of 17 amino acids from the human podocin sequence SKPVEPLNPKRKDSPML. For CD2AP, anti-CD2AP antibody (NI21-25) was prepared in rabbits immunized with whole molecules of CD2AP (fusion protein), and another rabbit anti-CD2AP antibody (SC9137) was purchased from Santa Cruz Biotechnology, Inc. This antibody recognizes the C-terminal end of CD2AP which binds to nephrin [23, 24]. The specificities of the antibody against the C-terminus of podocin and the anti-CD2AP antibody (NI21-25) were confirmed by Western blot analysis. The Western blot findings are shown in Figure 1. The staining patterns of nephrin, podocin, CD2AP, and α_3 integrin were evaluated in accordance with the method described in Experiment 1. The staining pattern of podocalyxin could not be evaluated by this method, because under careful observation it was found to be discontinuous even in normal glomeruli. In order to compare the localization of nephrin with that of podocin or CD2AP, dual-labeling immunofluorescence studies were carried out. In order to analyze the subcellular localization of nephrin and podocin, semiquantitative Western blot analysis with sequentially solubilized glomerular samples was carried out.

Experiment 3: Studies on active Heymann nephritis. Active Heymann nephritis was induced in nine male

Lewis rats by five immunizations with Fx1A, and four rats showing massive proteinuria were sacrificed 19 weeks after the first immunization. As a control group, three age-matched normal rats were sacrificed. Twenty-four–hour urine samples were collected every week after the first immunization. Kidney sections were used for the immunofluorescence study. The depositions of rat IgG and rat C3 were analyzed in accordance with the method described in Experiment 1. The stainings of nephrin, podocin, CD2AP, podocalyxin, and α_3 integrin were investigated with the antibodies described above. The staining patterns of nephrin, podocin, CD2AP, and α_3 integrin were scored by the same method as in Experiment 1. In order to compare the localization of nephrin with that of podocin or CD2AP, dual-labeling immunofluorescence studies were carried out. For the dual-labeling immunofluorescence studies, rabbit anti-CD2AP antibody (SC9137) was used.

Morphologic and immunohistochemical studies

Light and electron microscopic studies were performed according to the previously described methods [31, 32, 34]. For light microscopy, a section was stained with periodic acid-methenamine silver.

Immunofluorescence studies were performed according to the method previously described [41]. Renal tissue was quickly frozen in n-hexane cooled at -70°C. Three micrometer thick cryostat sections were fixed, incubated with the primary antibodies described above, and stained with FITC-conjugated antimouse IgG1 (Southern Biotechnology Associates, Inc., Birmingham, AL, USA) (for antinephrin monoclonal antibody 5-1-6, anti-α_3 integrin), FITC-conjugated antimouse IgG2a (Southern Biotechnology Associates) (for antipodocalyxin), or FITC-conjugated antirabbit immunoglobulins (Dako) (for antinephrin, antipodocin, and anti-CD2AP). For dual-labeling immunofluorescence analysis, tetramethyl rhodamine isothiocyanate (TRITC)-conjugated anti-mouse IgG1 (Southern Biotechnology Associates) was used to detect antinephrin monoclonal antibody 5-1-6. The species were observed with an immunofluorescence microscopy (BX50) (Olympus, Tokyo, Japan), or with a laser-scanning confocal microscopy (MRC-1024) (Bio-Rad) with the appropriate filter for FITC (488 nm excitation, HQ515/30 emission filter) and TRITC (568 nm excitation, 585LP filter). X-y and x-z scans were obtained. Images were further processed using Adobe Photoshop 6.0.
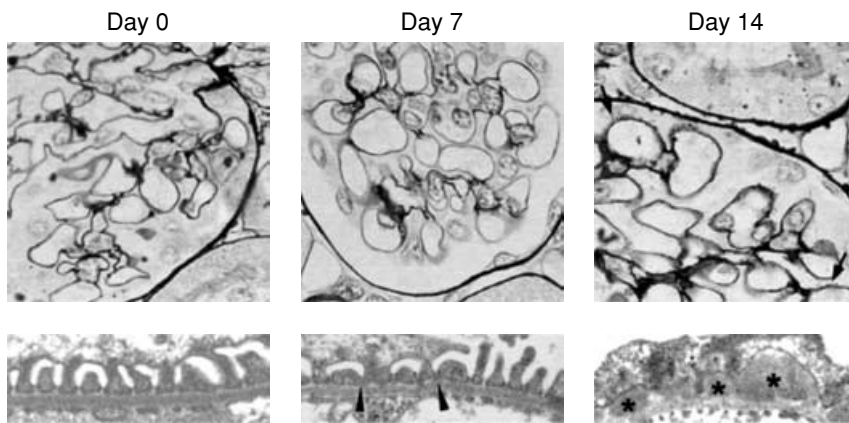
Semiquantitative Western blot analysis with sequentially solubilized glomerular lysates

Western blot analysis with sequentially solubilized glomerular lysates was performed basically according to

the method previously described [40]. Glomeruli from rats of passive Heymann nephritis sheep (days 0 and 7) were isolated with phosphate-buffered saline (PBS), including protease inhibitors. Ten thousand glomeruli of each sample were sequentially solubilized with 1% Triton X-100, RIPA buffer [0.1% SDS, 1% sodium deoxycholate, 1% Triton X-100, 0.15 mol/L NaCl, and 0.01 mol/L ethylenediaminetetraacetic acid (EDTA) in 0.025 mol/L Tris-HCl, pH 7.2] with protease inhibitors, and then separated into Triton X-100-soluble (T), RIPA-soluble (R), and RIPA-insoluble fractions. The RIPA-insoluble fraction was solubilized with SDS-PAGE sample buffer (2% SDS, 10% glycerol, and 5% 2-mercaproethanol in 0.0625 mol/L Tris-HCl, pH 6.8) (S fraction). Equal amounts of these sequentially solubilized fractions were subjected to SDS-PAGE with 7.5% or 10% acrylamide gel, according to the method of Laemmli [39] and transferred to a PVDF membrane (Bio-Rad) by electrophoretic transblotting for 30 minutes using Trans-Blot SD (Bio-Rad). After blocking with bovine serum albumin (BSA), the strips of membrane were exposed to rabbit antirat nephrin [32], rabbit antirat podocin [40], or rabbit antirat actin antibody purchased from Sigma-Aldrich (St. Louis, MO, USA). They were then washed and incubated with alkaline phosphatase–conjugated antirabbit immunoglobulins. The reaction was developed with an alkaline phosphatase chromogen kit. The density of the positive bands was quantitated by Densitograph (ATTO, Tokyo, Japan). This procedure was carried out twice. The percentage of the density of each fraction to the total was calculated. The percentage of the total amount of each molecule in passive Heymann nephritis sheep compared to the control group is shown in bar graphs as mean $\pm$ SD.

Real-time RT-PCR

Total RNA was extracted from isolated glomeruli by Trizol (Gibco BRL, Gaithersburg, MD, USA). cDNA was synthesized according to the method previously described [32, 40]. The primers of nephrin, podocin, and glyceraldehyde-3-phosphate dehydrogenase (GAPDH) were designed according to the published sequence [32, 40]. The primers of CD2AP were designed based on its sequence (GenBank AY205155) (CD2AP) (sense 5′-GAG GTA GAA GAA GGC TGG TGG AGT G-3′ and antisense 5′-CAG CCT GCT TCT CCA GTC TCC TT-3′). Real-time RT-PCR was performed with Takara Ex Taq R-PCR Version 1.0 (Takara, Otsu, Japan) and SYBR Green I (Takara), in accordance with the manufacturer's instructions. The template cDNA were amplified in a 25 μL total volume of PCR buffer containing 2.5 μL of 10 × R-PCR buffer (Mg^{2+} free), 0.00084 μL of SYBR Green I, 3 mmol/L MgCl$_2$, 0.3 mmol/L each deoxyadenosine triphosphate (dATP),

Day 0 Day 7 Day 14

deoxycytidimine triphosphate (dCTP), deoxyguanosine triphosphate (dGTP), and deoxythymidine triphosphate (dTTP), and 0.3 μmol/L of each of the 5′ and 3′ primers and 1.25 U of Takara Ex Taq HS. Two-step PCRs were run on a Smart Cycler System I (Takara) of denaturation at 95°C for 3 seconds, annealing at individual temperatures for 30 seconds. The reactions and runs were performed six times for each sample. PCR products of nephrin, podocin, CD2AP, and GAPDH were subcloned into the plasmid vector pCR II-TOPO (TOPO TA Cloning Kit Dual Promoter) (Invitrogen, Carlsbad, CA, USA). The plasmid DNAs subcloned with the PCR products were isolated and purified with a Plasmid Midi Kit (Qiagen, Hilden, Germany). The concentration of each plasmid was determined by measurements of the absorbance at 260 nm, and its copy number was calculated. In order to generate the calibration curves, the stock solutions were diluted from 10^4 to 10^9 copies/μL. The fluorescence intensity of 400 nmol/L FAM (carboxyfluorescein) was defined as 1000 U, and the threshold was set at 30 U of fluorescence intensity. The C_t value was defined as the cycle number at which the fluorescence intensity curve crosses this threshold. The calibration curve was plotted as C_t (x axis) versus the logarithm of the starting copy number (y axis).

RESULTS

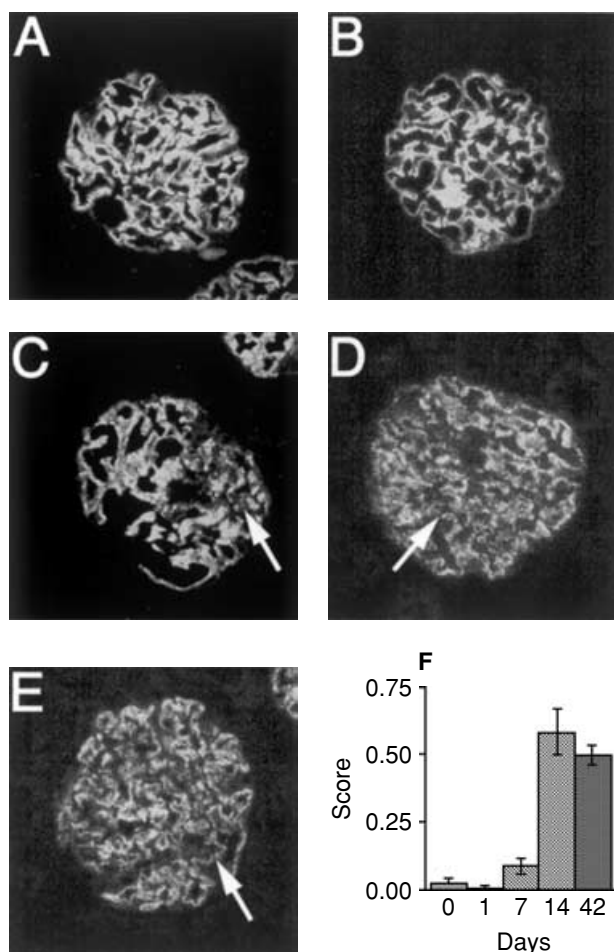### Experiment 1: Passive Heymann nephritis rabbit

Characterization of passive Heymann nephritis rabbit.
The amounts of urinary protein excretion on days 0, 7, 14, and 42 in passive Heymann nephritis rabbit were 3.5 ± 0.4, 5.3 ± 0.9, 238.5 ± 93.8, and 41.0 ± 14.3 mg/day, respectively. The deposition of rabbit IgG and rat C3 in the glomeruli was detected on day 1. The deposition of rat IgG was first detected on day 14 (data not shown). The light and electron microscopic findings in passive Heymann nephritis rabbit are shown in Figure 2. No extensive morphologic alteration was observed on day 7 in passive

Heymann nephritis rabbit, although a partial effacement of the podocyte foot processes was observed. Spike formations along the glomerular capillary wall were first detected on day 14. Subepithelial deposits and effacement of the podocyte foot processes were well noticeable on day 14.

Immunofluorescence stainings of podocyte-associated molecules in passive Heymann nephritis rabbit. The kinetics of the immunofluorescence stainings of nephrin detected by the murine antinephrin monoclonal antibody (5-1-6) in passive Heymann nephritis rabbit are shown in Figure 3. Nephrin staining was observed to have a linear pattern on day 0 and day 1 (Fig. 3A and B). Discontinuous staining of nephrin was observed in some glomeruli on day 7 (Fig. 3C), and in almost all the glomeruli on day 14 and day 42 (Fig. 3D and E). By contrast, no extensive alteration of the staining of α_3 integrin or podocalyxin was detected throughout the period examined (data not shown). The score for nephrin staining is summarized in Figure 3F.

Analysis of urinary nephrin and podocin in passive Heymann nephritis rabbit. The Western blot findings for nephrin in the urine samples are shown in Figure 4 (upper panel). Nephrin was detected as two bands of around 180 kD in glomerular lysate. A band of approximately 180 kD corresponding to the lower band of nephrin in glomerular lysate and other bands of around 200 kD were detected in urine samples from rats on day 7 of passive Heymann nephritis rabbit (lane 1). These bands were not detected in urine samples from normal rats (lane 3) or negative controls incubated with preimmune rabbit serum (lane 4). The Western blot findings for podocin are shown in Figure 4 (lower panel). Urinary podocin was detected neither on day 0, nor on day 7.

mRNA expression of slit diaphragm–associated molecules in passive Heymann nephritis-rabbit. The calibration curves are GAPDH, y = −0.301x + 12.301 ($r^2 = 0.998$); nephrin, y = −0.306x + 12.615 ($r^2 = 0.998$);
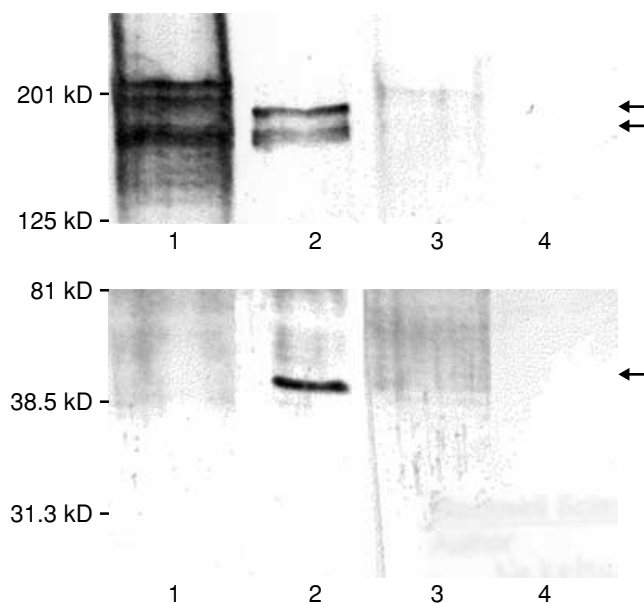
Fig. 3. Immunofluorescence findings for nephrin in passive Heymann nephritis induced by rabbit antifraction 1A (anti-Fx1A). Nephrin staining with monoclonal antibody 5-1-6 was observed to have a linear pattern on day 0 (*A*) and day 1 (*B*). Some glomeruli showed granular patterns on day 7 (*C*), when abnormal proteinuria was not observed yet. Most glomeruli showed granular patterns on day 14 (*D*) and day 42 (*E*). The kinetics of the nephrin staining score is shown in (*F*). The staining patterns of nephrin were evaluated using the method described in the **Methods** section.

Fig. 4. Western blot analyses of urinary nephrin and podocin in passive Heymann nephritis induced by rabbit antifraction 1A (anti-Fx1A). Urinary nephrin was examined by Western Blot analysis in passive Heymann nephritis rabbit (upper panel). Nephrin was detected as two bands of around 180 kD in glomerular lysate (lane 2, arrows). A band of around 180 kD corresponding to the lower band of nephrin of glomerular lysate and other bands of around 200 kD were detected in the urine samples of rats on day 7 of passive Heymann nephritis rabbit (lane 1). These bands were not detected in urine samples from normal rats (lane 3) or negative controls incubated with preimmune rabbit serum (lane 4). The lower panel shows the Western Blot findings for podocin in the urine samples. A podocin band of approximately 42 kD was detected in the glomerular lysate. Urinary podocin was not detected on day 0 (lane 3) or day 7 (lane 1). Lanes 1 and 4 show the urine of rats on day 7 of passive Heymann nephritis rabbit. Lane 2 is the glomerular lysate (positive control). Lane 3 is the urine of control rats (day 0). Lanes 1 to 3 were exposed to antinephrin antibody (upper panel) or antipodocin antibody (lower panel). Lane 4 was exposed to preimmune rabbit serum.

podocin, $y = -0.319x + 12.796$ ($r^2 = 1.000$); and CD2AP, $y = -0.283x + 11.169$ ($r^2 = 0.999$). The copy numbers of mRNA for nephrin, podocin, and CD2AP per 10^8 copies of GAPDH mRNA in the early phase of passive Heymann nephritis rabbit (days 0, 1, and 7) are shown in Figure 5. Glomerular mRNA expressions of nephrin decreased to 46.8% on day 1 and 24.0% on day 7. Glomerular mRNA expressions of podocin decreased to 44.2% on day 1 and 24.1% on day 7. A slight decrease of mRNA expression of CD2AP was detected on day 7 (67.3%).

## Experiment 2: Passive Heymann nephritis sheep

Characterization of passive Heymann nephritis sheep. The amounts of urinary protein excretion in passive Hey-

mann nephritis caused by sheep anti-Fx1A (passive Heymann nephritis sheep) on days 0, 4, and 7 were 2.1 ± 0.4, 7.5 ± 3.6, and 83.5 ± 8.8 mg/day, respectively.

Immunofluorescence stainings of podocyte-associated molecules in passive Heymann nephritis sheep. The immunofluorescence findings of podocyte-associated molecules on day 7 of passive Heymann nephritis sheep are shown in Figure 6. Not only nephrin, but also podocin and CD2AP staining shifted to a discontinuous pattern on day 7 of passive Heymann nephritis sheep. By contrast, no extensive alteration of the staining of podocalyxin or α_3 integrin was detected from the control to the passive Heymann nephritis sheep. For staining of nephrin, podocin and CD2AP, two antibodies against each molecule were used. For each molecule, no difference in staining was detected between the two antibodies. The scores for the distribution of podocyte-associated molecules in passive Heymann nephritis sheep are shown in Figure 6 (lower panel).
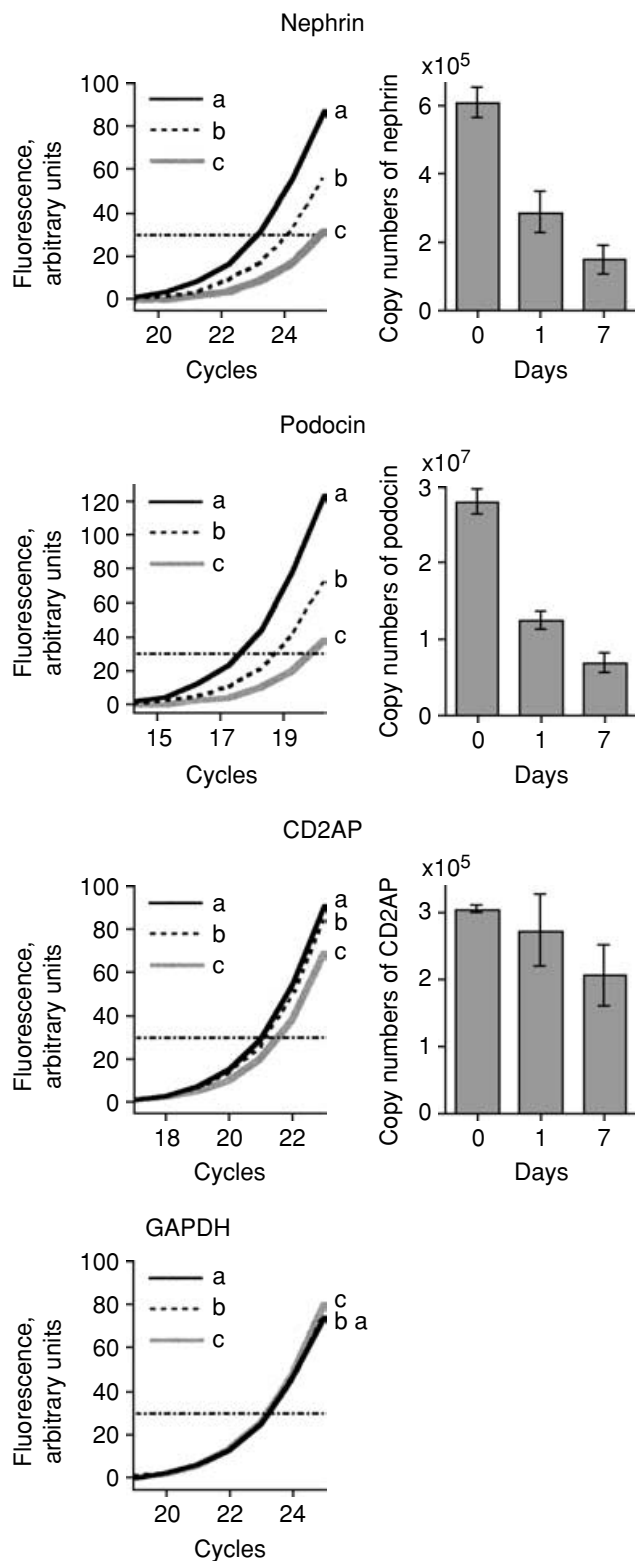
Fig. 5. Real-time reverse transcription-polymerase chain reaction (RT-PCR) analysis of slit diaphragm–associated molecules in the glomeruli of passive Heymann nephritis induced by rabbit antifraction 1A (anti-Fx1A). The left panel shows the fluorescence intensity of the RT-PCR analyses of nephrin, podocin, CD2AP, and glyceraldehyde-3-phosphate dehydrogenase (GAPDH). The x axis shows the number of PCR cycles, and the y-axis shows the fluorescence intensity. The lines in the graphs are: a, passive Heymann nephritis day 0; b, passive Heymann nephritis day 1; and c, passive Heymann nephritis day 7. Dot-dash lines indicate the threshold that was set at 30 U of fluorescence intensity. The right panel shows the copy numbers of mRNA for nephrin, podocin and CD2AP per 10^8 copies of GAPDH mRNA. The copy numbers were determined using the calibration curves. The PCR reactions and runs were performed six times per each sample. The columns represent mean values of six examinations, and the bars show 1 standard deviation. Glomerular mRNA levels of nephrin and podocin were clearly reduced on day 7 of passive Heymann nephritis rabbit.

The dual-labeling results for nephrin with podocin and CD2AP in passive Heymann nephritis sheep are shown in Figure 7. A merged image of nephrin with podocin shows a yellow pattern in control rats (Fig. 7B). The stainings patterns of podocin and nephrin shifted to granular in passive Heymann nephritis sheep, but the shifts of these proteins were not parallel (Fig. 7E). Confocal microscopic studies also showed podocin and nephrin were dissociated in passive Heymann nephritis sheep (day 7) (Fig. 7N). The staining patterns of CD2AP and nephrin were linear in the control rats. Although the staining patterns of CD2AP and nephrin were not completely coincident, they were very similar in the control rats (Fig. 7H). In the glomeruli of rats with passive Heymann nephritis sheep, nephrin and CD2AP were redistributed, and some portions of the nephrin staining were clearly divergent from those of CD2AP (Fig. 7K).
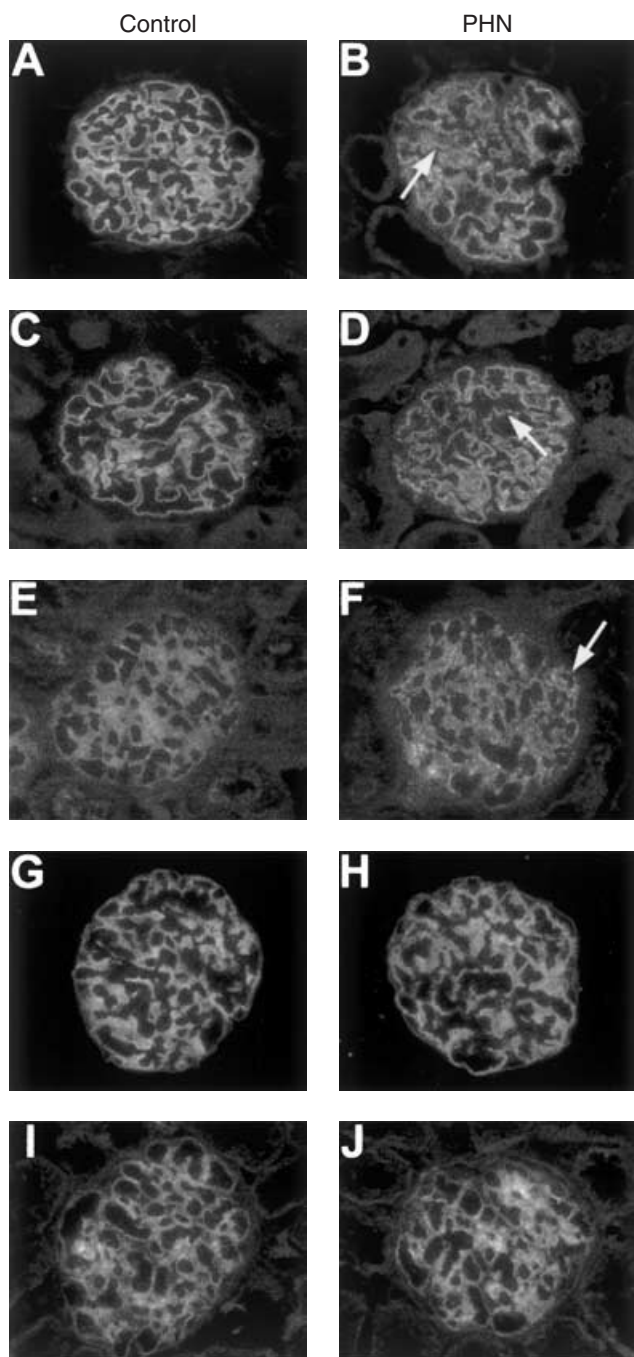
Semiquantitative Western blot analysis with sequentially solubilized glomerular lysates. The amounts of nephrin and podocin and their subcellular localization were analyzed by Western blot analysis with sequentially solubilized glomerular lysates in passive Heymann nephritis sheep (Fig. 8). Nephrin was detected as two bands in some fractions. However, the intensities of two bands were quantified together, because the lower band was very weak. The total amount of nephrin and podocin clearly decreased ($52.9 \pm 12.4\%$ and $62.7 \pm 17.7\%$ to normal, respectively), although the amount of actin did not change (represented as bar graphs). The ratio of the amount of nephrin in the Triton X-100 soluble fraction to the total amount of nephrin increased in the proteinuric state (passive Heymann nephritis sheep 59.7% versus control 39.7%), although the distribution of podocin in the fractions remained unchanged (passive Heymann nephritis sheep 28.8% versus control 28.4%).

Experiment 3: Active Heymann nephritis

Characterization of active Heymann nephritis. On week 19 of active Heymann nephritis, spike formations along the glomerular capillary wall were observed by light microscopy, and subepithelial deposits were observed by electron microscopy (data not shown). Deposition of rat IgG and C3 was observed in the glomeruli of active Heymann nephritis rats (data not shown). Abnormal

Control   PHN

proteinuria was first detected 10 weeks after the first immunization in four out of nine rats (57.0 ± 23.8 mg/24 hours). These rats had massive proteinuria (516 ± 411 mg/24 hours) at the time of their death (19 weeks after the first immunization).

Immunofluorescence stainings of podocyte-associated molecules in active Heymann nephritis. The immunofluorescence findings for the slit diaphragm–associated molecules nephrin, podocin, and CD2AP, and the other podocyte-associated molecules podocalyxin and α_3 integrin on week 19 of active Heymann nephritis are shown in Figure 9. Shifts in the staining patterns of the slit diaphragm–associated molecules nephrin, podocin, and CD2AP were also observed in active Heymann nephritis (Fig. 9B, D, and F). In active Heymann nephritis, the staining intensity of podocalyxin decreased (Fig. 9H). No differences were detected in the staining of α_3 integrin between the control and active Heymann nephritis (Fig. 9J). For the staining of nephrin, podocin, and CD2AP, two antibodies against each molecule were used. No difference in staining was detected between the two antibodies of each molecule. The scores for the distribution of podocyte-associated molecules in active Heymann nephritis are shown in Figure 9 (lower panel).

The dual-labeling results of nephrin with podocin and CD2AP in active Heymann nephritis are shown in Figure 10. Nephrin-podocin dissociation was also observed in active Heymann nephritis (Fig. 10E and N). Although the staining patterns of CD2AP and nephrin were very similar in control rats (Fig. 10H), some portions of the nephrin staining were clearly divergent from those of CD2AP (Fig. 10K) in the glomeruli of active Heymann nephritis rats.
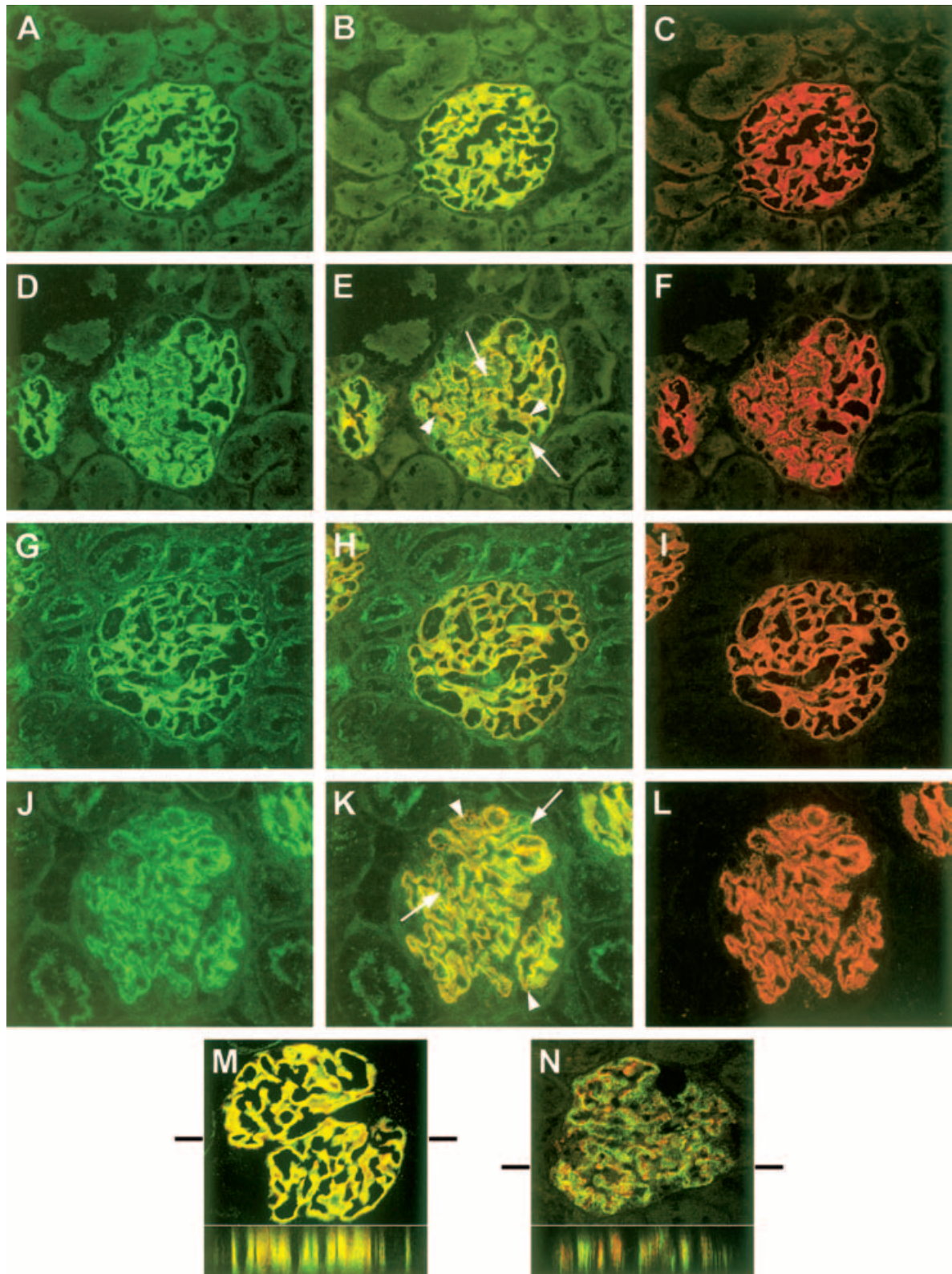
DISCUSSION

The kinetics of nephrin staining in passive Heymann nephritis induced in rats by rabbit anti-Fx1A antibody

Fig. 7. Dual-labeling results for podocin and CD2AP with nephrin in passive Heymann nephritis induced by sheep antifraction 1A (anti-Fx1A) (day 7). (*A to F*) The cryostat sections were incubated with rabbit antirat podocin antibody against the N-terminus of podocin, fluorescein isothiocyanate (FITC)-conjugated antirabbit immunoglobulins, antirat nephrin monoclonal antibody 5-1-6, and TRITC-conjugated antimouse IgG1, in that order. The localizations of podocin [green staining (A and D)] and nephrin [red staining (C and F)], and the double-exposure findings (B and E) are shown. The stainings patterns of podocin (A) and nephrin (C) were linear in control rats. A merged image of podocin and nephrin (B) shows yellow
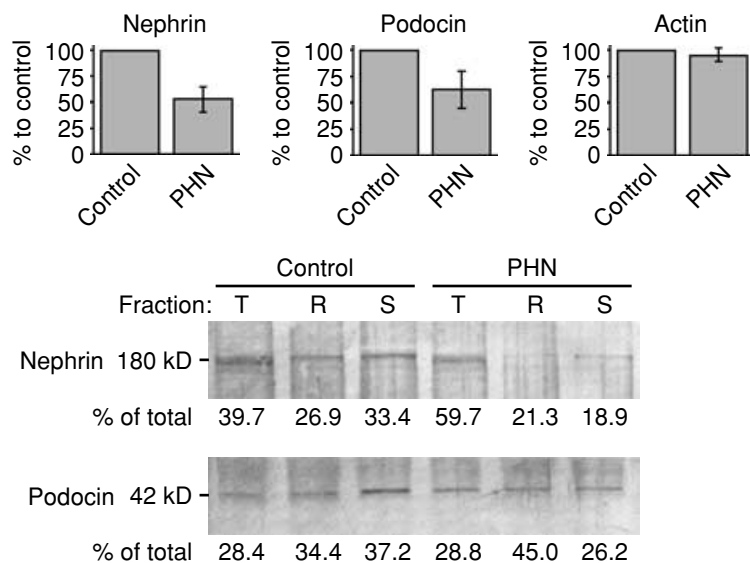
Fig. 8. Western blot analyses of the sequentially solubilized glomerular proteins with antinephrin and antipodocin antibodies in passive Heymann nephritis induced by sheep antifraction 1A (anti-Fx1A) (day 7). The amounts of nephrin and podocin and their subcellular localization were analyzed by Western blot analysis with sequentially solubilized glomerular lysates. Isolated glomeruli from normal and rats with passive Heymann nephritis sheep (day 7) were sequentially solubilized with Triton X-100, RIPA buffer, and sodium dodecyl sulfate-polyacrylamide gel electrophoresis (SDS-PAGE) sample buffer. Equal amounts of these sequentially solubilized fractions were loaded onto a polyacrylamide gel, electrophoresed, and then transferred to a polyvinylidine difluoride (PVDF) membrane. The membrane was incubated with rabbit antinephrin antibody, rabbit antipodocin antibody, or rabbit antiactin antibody, followed by alkaline phosphatase–conjugated anti-rabbit immunoglobulins. Abbreviations are: T, Triton X-100 soluble fractions; R, Triton X-100-insoluble and RIPA buffer soluble fractions; S, RIPA buffer insoluble and SDS-PAGE sample buffer soluble fractions. The densities of the positive bands were quantified. The percentages of the total amount of each molecule in rats with passive Heymann nephritis sheep compared to those in the control rats are shown in the bar graphs as mean ± SD. In rats with passive Heymann nephritis sheep on day 7, the total amounts of nephrin and podocin clearly decreased (52.9 ± 12.4% and 62.7 ± 17.7% to the control level, respectively; upper panel). The percentages of the amount of each fraction to the total are shown below the bands. The ratio of the amount of nephrin in the Triton X-100 soluble fractions to the total amount of nephrin increased in passive Heymann nephritis sheep (59.7%) and control (39.7%), although the distribution of podocin in the fractions remained unchanged (lower panel).

was analyzed using a murine monoclonal antinephrin antibody (5-1-6) which recognizes the extracellular site of rat nephrin [31–33]. The staining pattern of nephrin was already disrupted in some glomeruli on day 7, when neither abnormal proteinuria nor spike formation had yet been detected. Nephrin staining clearly shifted to a discontinuous granular pattern on day 14, when se-

vere proteinuria was observed (Fig. 3). These findings are compatible with previous reports [13, 14, 42]. We also analyzed the staining of podocin and CD2AP as well as nephrin in passive Heymann nephritis rabbit. Since some antibodies used for detecting these slit diaphragm–associated molecules are rabbit antibodies and are not available in passive Heymann nephritis rabbit, we

staining in control rats. The staining patterns of podocin (D) and nephrin (F) shifted to granular in passive Heymann nephritis sheep (day 7), but the shifts of these molecules were not parallel (merged image) (E). Podocin and nephrin did not always colocalize in passive Heymann nephritis sheep (arrows are green staining; arrow heads are red staining). (*G* to *L*) The sections were incubated with rabbit antirat CD2AP antibody (NI21-25), FITC-conjugated antirabbit immunoglobulins, antirat nephrin monoclonal antibody 5-1-6, and TRITC-conjugated antimouse IgG1, in that order. The localizations of CD2AP [green staining (G and J)] and nephrin [red staining (I and L)], and the double-exposure findings (H and K) are shown. The staining patterns of CD2AP (G) and nephrin (I) were linear in control rats. The staining patterns of CD2AP and nephrin were very similar (merged image) (H). The stainings of CD2AP (J) and nephrin (L) suffered redistribution in passive Heymann nephritis sheep (day 7). A merged image of CD2AP with nephrin (K) shows that some portions of the nephrin staining clearly diverge from the CD2AP staining in passive Heymann nephritis sheep (arrows are green staining; arrow heads are red staining). (*M* and *N*) Confocal microscopic findings of the merged image of podocin and nephrin. The dual-label staining was done as described (A to F). The localizations of podocin (green staining) and nephrin (red staining) in the horizontal sections (upper panel) and in the vertical sections (lower panel) are shown. Nephrin and podocin colocalized in control rats (M). In passive Heymann nephritis sheep, podocin (green staining) and nephrin (red staining) are clearly dissociated (N).
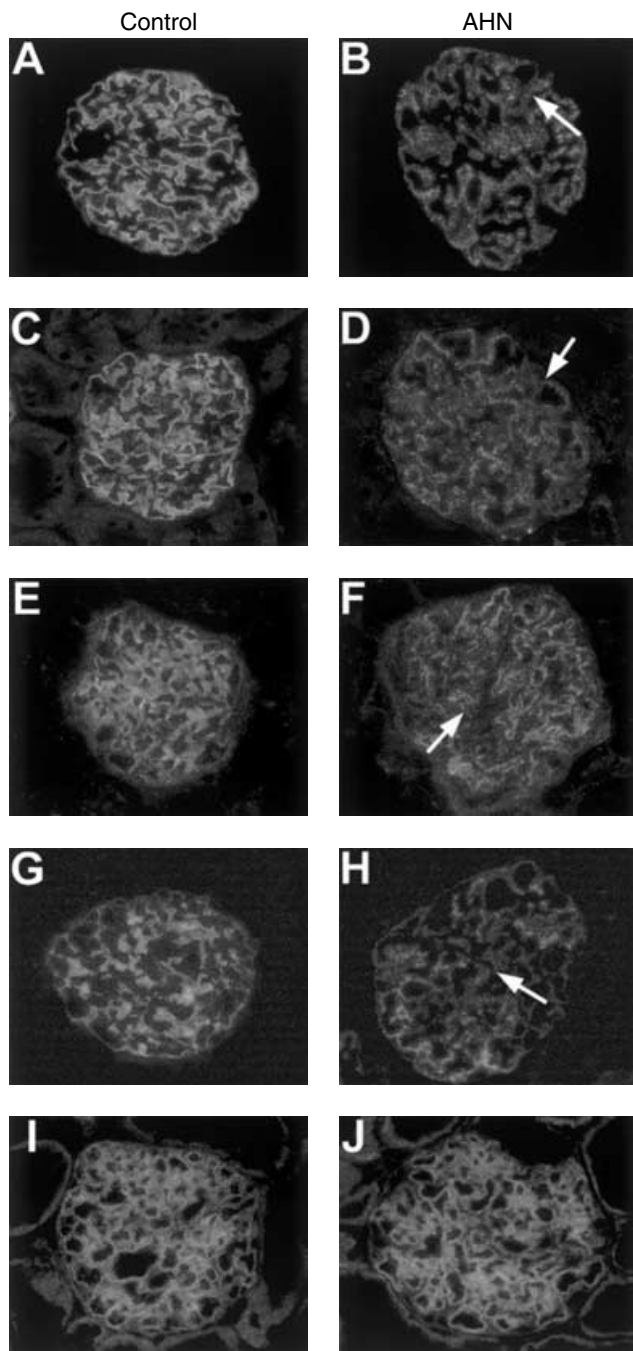
prepared passive Heymann nephritis sheep. We observed that the staining patterns of all of these slit diaphragm–associated molecules shifted to discontinuous in the proteinuric stage of this passive Heymann nephritis model (Fig. 6B, D, and F). In this study, we found that the staining pattern of CD2AP was altered in passive Heymann nephritis sheep, although our group previously reported that the staining intensity of CD2AP did not diminish [13]. No extensive alteration of podocalyxin or α_3 integrin was detected in passive Heymann nephritis rabbit (data not shown) or in passive Heymann nephritis sheep (Fig. 6). $\alpha_3\beta_1$ integrin plays a major role in connecting the basal side of podocyte to the glomerular basement membrane [35–37]. Podocalyxin is a podocyte apical membrane molecule with a negative charge [43]. It is believed that podocalyxin plays a role in maintaining the highly differentiated structure of the podocyte, with its interdigitating foot processes [44, 45]. The findings obtained here may indicate that alterations in the expression of slit diaphragm–associated molecules which are essential for the development of proteinuria, rather than the alteration of the apical and basal molecules of the podocyte. The stainings of nephrin, podocin, and CD2AP were analyzed with the help of two antibodies against each molecule, and no differences in the findings between the two antibodies for each molecule were detected. This strongly suggests that the shifts in the staining patterns are due not to the alteration of a portion of these molecules, but to the alteration of the whole molecule. In order to further analyze the etiological significance of the alteration of slit diaphragm components, we analyzed the mRNA expression of slit diaphragm–associated molecules (nephrin, podocin, and CD2AP) at the early stages of this model (Fig. 5). We found that the mRNA expression of nephrin and podocin decreased prior to the onset of proteinuria. These findings show that there is decreased synthesis of slit diaphragm components, which likely contributes to the reduction in slit diaphragm protein levels. These changes may initiate the onset of proteinuria. All of these

Fig. 9. Immunofluorescence findings for podocyte-associated molecules in active Heymann nephritis. The nephrin staining with monoclonal antibody 5-1-6 (*A* and *B*), podocin staining with rabbit antibody against the N-terminus of podocin (*C* and *D*), CD2AP staining with anti-CD2AP antibody (NI21-25) (*E* and *F*), podocalyxin staining with monoclonal antipodocalyxin antibody (*G* and *H*), and α_3 integrin staining with monoclonal antibody against α_3 integrin (*I* and *J*) are shown. The staining patterns of nephrin (A), podocin (C), and CD2AP (E) were linear in control rats. The staining patterns of nephrin (B), podocin (D) and CD2AP (F) were granular (arrow) in active Heymann nephritis. (G) The staining of podocalyxin in normal rats. The staining intensity of podocalyxin was diminished (arrows) in active Heymann nephritis (H). No differences were detected in the staining of α_3 integrin between the control (I) and active Heymann nephritis (J). The lower panel shows the staining scores for nephrin, podocin, CD2AP, and α_3 integrin. The staining patterns were scored in accordance with the method described in the **Methods** section.
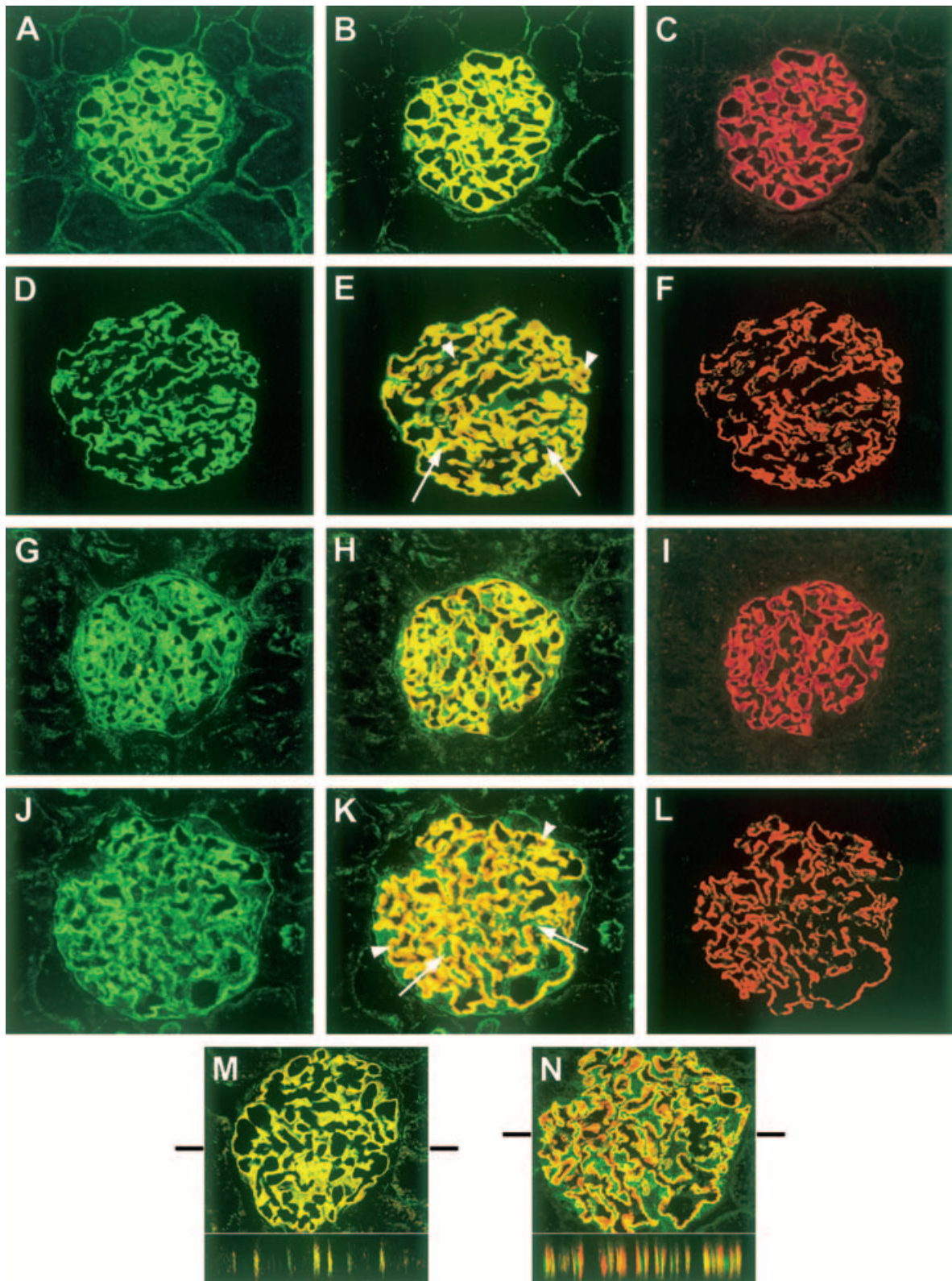
Fig. 10. Dual-labeling results for podocin and CD2AP with nephrin in active Heymann nephritis. (*A* to *F*) The cryostat sections were incubated with rabbit antirat podocin antibody against the N-terminus of podocin, fluorescein isothiocyanate (FITC)-conjugated antirabbit immunoglobulins, antirat nephrin monoclonal antibody 5-1-6, and TRITC-conjugated anti-mouse IgG1, in that order. The localizations of podocin [green staining (A and D)] and nephrin [red staining (C and F)], and the double-exposure findings (B and E) are shown. The staining patterns of podocin (A) and nephrin (C) were linear in control rats. A close proximity between podocin and nephrin is observed in normal rat glomeruli (merged image) (B).

results indicate that the molecular rearrangement of the slit diaphragm components is essential for the development of proteinuria in passive Heymann nephritis.

Some recent studies have shown by pull-down assay that nephrin interacts with podocin [19, 20] and CD2AP [21], and other studies have shown that podocin plays a part in the recruitment of nephrin into the slit pore of the podocyte [22, 46]. It has also been reported that nephrin-induced signals are enhanced by podocin [20, 46]. These studies indicate that the interaction of these slit diaphragm–associated molecules is essential in maintaining slit diaphragm function. Therefore, in order to analyze the alteration of the interaction of nephrin with podocin and CD2AP, we investigated the localization of nephrin, podocin, and CD2AP with dual-labeling immunofluorescence techniques. A close proximity between nephrin and podocin was observed in normal rat glomeruli, but the localizations of these molecules were not coincident in the glomeruli of proteinuric rats with passive Heymann nephritis sheep (Fig. 7). Nephrin and CD2AP showed very similar linear staining patterns along the glomerular capillary wall, although their localizations were not completely coincident even in normal rat glomeruli. We observed that nephrin and CD2AP were redistributed in passive Heymann nephritis sheep, and a portion of the nephrin staining was clearly divergent from that of CD2AP (Fig. 7). These findings indicate that the altered interaction of the slit diaphragm components, as well as the decreased expression of these molecules, may contribute to the development of proteinuria in this model of membranous nephropathy.

In this study, the subcellular localizations of nephrin and podocin in proteinuric glomeruli were also analyzed by Western blotting with sequentially solubilized materials (Fig. 8). We previously reported that the Triton X-100 soluble fraction was rich in nephrin, and that nephrin was also found in the Triton X-100 insoluble/RIPA soluble fraction and the RIPA insoluble fraction of normal rat glomeruli. By contrast, podocin is mainly found in the Triton X-100 insoluble/RIPA soluble and the RIPA insoluble fractions [40]. In this study, we analyzed whether nephrin and podocin-rich fractions shift in the pathogenic glomeruli of rats with

passive Heymann nephritis sheep. We found that the ratio of the amount of nephrin in the Triton X-100 soluble fraction to that of the total amount of nephrin was elevated in passive Heymann nephritis sheep, whereas no such shift was detected in podocin. These results indicate that nephrin became more soluble in the mild detergent, while podocin did not. The detergent resistance of membrane proteins is related to their association with the cytoskeleton and/or detergent-resistant lipid rafts. Nephrin is associated with the cytoskeleton and resides partly in lipid rafts [47]. It can be solubilized by disrupting F-actin, whereas podocin is solubilized by dissolving the lipid rafts [19]. Thus, the most plausible explanation for the relative increase in the solubility of nephrin but not of podocin in passive Heymann nephritis is that podocyte injury causes nephrin to dissociate from podocin and the actin cytoskeleton [13].

We have shown here that urinary nephrin is found in passive Heymann nephritis rabbit (Fig. 4). Although Patari et al [48] reported that some small fragments of nephrin were detected in patients with diabetes, some studies reported that nephrin bands of 180 ∼ 160 kD were detected in the urine of proteinuric rats [49, 50]. We detected a nephrin band of around 180 kD, which corresponds to the lower band of glomerular lysate, in the urine of rats with passive Heymann nephritis rabbit. It is not clear that the nephrin detected in this urine is membrane-associated, since Simons et al [51] reported that the upper band of nephrin is membrane-associated and the lower band is endoplasmic reticulum–associated. We also detected some other bands around 200 kD in urine samples of rats with passive Heymann nephritis rabbit. Although we cannot clearly explain the characteristics of these bands, we think that they might be proteins aggregated with nephrin. Our Western blot study with sequentially solubilized glomerular lysate showed that the solubility of nephrin increased, whereas that of podocin did not. Podocin was not detected in the urine samples in which nephrin was detected. These findings suggest that it is conceivable that the membrane-associated nephrin was dissociated from podocin and excreted into the urine, although we have not fully understood the characteristics of each band of nephrin. Also, we would like to

---

The stainings patterns of podocin (D) and nephrin (F) shifted to granular in active Heymann nephritis, but the shifts of these molecules were not parallel (merged image) (E). Podocin and nephrin did not always colocalize in active Heymann nephritis (arrows are green staining; arrow heads are red staining). (*G* to *L*) The sections were incubated with rabbit antirat CD2AP antibody (SC9137), FITC-conjugated antirabbit immunoglobulins, antirat nephrin monoclonal antibody 5-1-6, and TRITC-conjugated antimouse IgG1, in that order. The localizations of CD2AP [green staining (G and J)] and nephrin [red staining (I and L)], and the double-exposure findings (H and K) are shown. The staining patterns of CD2AP (G) and nephrin (I) were linear in control rats. The staining patterns of CD2AP (J) and nephrin (L) shifted to granular in active Heymann nephritis. A merged image of CD2AP with nephrin (K) shows that some portions of the nephrin staining are clearly divergent from the CD2AP staining in active Heymann nephritis (arrows are green staining; arrow heads are red staining). (*M* and *N*) Confocal microscopic findings of a merged image of podocin and nephrin. The dual-label staining was done as described (A to F). The localizations of podocin (green staining) and nephrin (red staining) in the horizontal sections (upper panel) and in the vertical sections (lower panel) are shown. Nephrin and podocin colocalized in control rats (M). Podocin and nephrin are clearly dissociated in active Heymann nephritis (N).

emphasize that urinary nephrin was detected on day 7 of passive Heymann nephritis rabbit, when no abnormal proteinuria was detected yet. Patari et al [48] also reported that urinary nephrin was present in normoalbuminuric patients with type 1 diabetes. These findings suggest that urinary nephrin may be of additional diagnostic value in our understanding of podocyte injury.

Alterations in nephrin, podocin, and CD2AP staining were also detected in active Heymann nephritis. To our knowledge, no better model than passive Heymann nephritis and active Heymann nephritis has been designed to date, although it is thought that major epitopes causing passive Heymann nephritis do not exist in humans [52]. We believe that these experimental models are accepted as important for the analysis of the pathogenesis of idiopathic membranous nephropathy. In this study, we observed the molecular rearrangement of the slit diaphragm components in both active Heymann nephritis and passive Heymann nephritis. The results may suggest that slit diaphragm dysfunction is connected with the development of proteinuria in human membranous nephropathy.

CONCLUSION

In this study, we have demonstrated that alterations in the expression and localization of slit diaphragm–associated molecules are essential for the development of proteinuria in experimental models of membranous nephropathy. Immunofluorescence studies showed that the staining patterns of nephrin, podocin, and CD2AP already shifted from linear to granular in the early phases of passive Heymann nephritis. Dual-labeling immunofluorescence studies and Western blot analysis with sequentially solubilized glomerular lysate showed that nephrin and podocin do not colocalize in the proteinuric state of either passive Heymann nephritis or active Heymann nephritis. Real-time RT-PCR studies showed that the expressions of nephrin and podocin decreased prior to the onset of proteinuria of passive Heymann nephritis rabbit. Urinary nephrin was detected on day 7 of passive Heymann nephritis rabbit when no abnormal proteinuria, whereas podocin was not. These results indicate that the reduced expression of nephrin and podocin, along with their dissociation may contribute to the development of proteinuria in membranous nephropathy.

ACKNOWLEDGMENTS

Reprint requests to Hiroshi Kawachi, M.D., Ph.D., Department of Cell Biology, Institute of Nephrology, Niigata University Graduate School of Medical and Dental Sciences, 1-757 Asahimachi-dori, 951-8510, Niigata, Japan.
E-mail: kawachi@med.niigata-u.ac.jp

REFERENCES

1. COUSER WG, ABRASS CK: Pathogenesis of membranous nephropathy. *Annu Rev Med* 39:517–530, 1988
2. KESTILA M, LENKKERI U, MANNIKKO M, *et al*: Positionally cloned gene for a novel glomerular protein–nephrin–is mutated in congenital nephrotic syndrome. *Mol Cell* 1:575–582, 1998
3. RUOTSALAINEN V, LJUNGBERG P, WARTIOVAARA J, *et al*: Nephrin is specifically located at the slit diaphragm of glomerular podocytes. *Proc Natl Acad Sci USA* 96:7962–7967, 1999
4. DOUBLIER S, RUOTSALAINEN V, SALVIDIO G, *et al*: Nephrin redistribution on podocytes is a potential mechanism for proteinuria in patients with primary acquired nephrotic syndrome. *Am J Pathol* 158:1723–1731, 2001
5. WANG SX, RASTALDI MP, PATARI A, *et al*: Patterns of nephrin and a new proteinuria-associated protein expression in human renal diseases. *Kidney Int* 61:141–147, 2002
6. KIM BK, HONG HK, KIM JH, LEE HS: Differential expression of nephrin in acquired human proteinuric diseases. *Am J Kidney Dis* 40:964–973, 2002
7. PATRAKKA J, RUOTSALAINEN V, KETOLA I, *et al*: Expression of nephrin in pediatric kidney diseases. *J Am Soc Nephrol* 12:289–296, 2001
8. SALANT DJ, QUIGG RJ, CYBULSKY AV: Heymann nephritis: Mechanism of renal injury. *Kidney Int* 35:976–984, 1989
9. EDGINGTON TS, GLASSOCK RJ, DIXON FJ: Autologous immune complex nephritis induced with renal tubular antigen. I. Identification and isolation of the pathogenetic antigen. *J Exp Med* 127:555–572, 1968
10. SUGISAKI T, KLASSEN J, ANDRES GA, *et al*: Passive transfer of Heymann nephritis with serum. *Kidney Int* 3:66–73, 1973
11. BARABAS AZ, LANNIGAN R: Induction of an autologous immune-complex glomerulonephritis in the rat by intravenous injection of heterologous anti-rat kidney tubular antibody. I. Production of chronic progressive immune-complex glomerulonephritis. *Br J Exp Pathol* 55:47–55, 1974
12. BRENTJENS JR, ANDRES G: Interaction of antibodies with renal cell surface antigens. *Kidney Int* 35:954–968, 1989
13. YUAN H, TAKEUCHI E, TAYLOR GA, *et al*: Nephrin dissociates from actin, and its expression is reduced in early experimental membranous nephropathy. *J Am Soc Nephrol* 13:946–956, 2002
14. FUJIGAKI Y, BATSFORD S, YAMASHITA F, *et al*: Sequence of events in the glomerular capillary wall at the onset of proteinuria in passive Heymann nephritis. *Virchows Arch* 438:136–145, 2001
15. BOUTE N, GRIBOUVAL O, ROSELLI S, *et al*: NPHS2, encoding the glomerular protein podocin, is mutated in autosomal recessive steroid-resistant nephrotic syndrome. *Nat Genet* 24:349–354, 2000
16. ROSELLI S, GRIBOUVAL O, BOUTE N, *et al*: Podocin localizes in the kidney to the slit diaphragm area. *Am J Pathol* 160:131–139, 2002
17. SHIH NY, LI J, KARPITSKII V, *et al*: Congenital nephrotic syndrome in mice lacking CD2-associated protein. *Science* 286:312–315, 1999
18. SELLIN L, HUBER TB, GERKE P, *et al*: NEPH1 defines a novel family of podocin interacting proteins. *FASEB J* 17:115–117, 2003
19. SCHWARZ K, SIMONS M, REISER J, *et al*: Podocin, a raft-associated component of the glomerular slit diaphragm, interacts with CD2AP and nephrin. *J Clin Invest* 108:1621–1629, 2001
20. HUBER TB, KOTTGEN M, SCHILLING B, *et al*: Interaction with podocin facilitates nephrin signaling. *J Biol Chem* 276:41543–41546, 2001
21. HUBER TB, HARTLEBEN B, KIM J, *et al*: Nephrin and CD2AP associate with phosphoinositide 3-OH kinase and stimulate AKT-dependent signaling. *Mol Cell Biol* 23:4917–4928, 2003
22. HUBER TB, SIMONS M, HARTLEBEN B, *et al*: Molecular basis of the functional podocin-nephrin complex: mutations in the NPHS2 gene disrupt nephrin targeting to lipid raft microdomains. *Hum Mol Genet* 12:3397–3405, 2003

23. Shih NY, Li J, Cotran R, et al: CD2AP localizes to the slit diaphragm and binds to nephrin via a novel C-terminal domain. *Am J Pathol* 159:2303–2308, 2001

24. Palmen T, Lehtonen S, Ora A, et al: Interaction of endogenous nephrin and CD2-associated protein in mouse epithelial M-1 cell line. *J Am Soc Nephrol* 13:1766–1772, 2002

25. Saleem MA, Ni L, Witherden I, et al: Co-localization of nephrin, podocin, and the actin cytoskeleton: Evidence for a role in podocyte foot process formation. *Am J Pathol* 161:1459–1466, 2002

26. Li C, Ruotsalainen V, Tryggvason K, et al: CD2AP is expressed with nephrin in developing podocytes and is found widely in mature kidney and elsewhere. *Am J Physiol Renal Physiol* 279:F785–F792, 2000

27. Ruotsalainen V, Patrakka J, Tissari P, et al: Role of nephrin in cell junction formation in human nephrogenesis. *Am J Pathol* 157:1905–1916, 2000

28. Edgington TS, Glassock RJ, Watson JI, Dixon FJ: Characterization and isolation of specific renal tubular epithelial antigens. *J Immunol* 99:1199–1210, 1967

29. de Heer E, Daha MR, van Es LA: Lymph node cells from rats with Heymann's nephritis produce in vitro autoantibodies directed against purified renal tubular antigen. *Immunology* 52:743–752, 1984

30. Salant DJ, Cybulsky AV: Experimental glomerulonephritis. *Method Enzymol* 162:421–461, 1988

31. Orikasa M, Matsui K, Oite T, Shimizu F: Massive proteinuria induced in rats by a single intravenous injection of a monoclonal antibody. *J Immunol* 141:807–814, 1988

32. Kawachi H, Koike H, Kurihara H, et al: Cloning of rat nephrin: Expression in developing glomeruli and in proteinuric states. *Kidney Int* 57:1949–1961, 2000

33. Topham PS, Kawachi H, Haydar SA, et al: Nephritogenic mAb 5-1-6 is directed at the extracellular domain of rat nephrin. *J Clin Invest* 104:1559–1566, 1999

34. Han GD, Koike H, Nakatsue T, et al: IFN-inducible protein-10 has a differential role in podocyte during Thy 1.1 glomerulonephritis. *J Am Soc Nephrol* 14:3111–3126, 2003

35. Kerjaschki D, Ojha PP, Susani M, et al: A beta 1-integrin receptor for fibronectin in human kidney glomeruli. *Am J Pathol* 134:481–489, 1989

36. Korhonen M, Ylanne J, Laitinen L, Virtanen I: The alpha 1-alpha 6 subunits of integrins are characteristically expressed in distinct segments of developing and adult human nephron. *J Cell Biol* 111:1245–1254, 1990

37. Adler S: Characterization of glomerular epithelial cell matrix receptors. *Am J Pathol* 141:571–578, 1992

38. Macconi D, Ghilardi M, Bonassi ME, et al: Effect of angiotensin-converting enzyme inhibition on glomerular basement membrane permeability and distribution of zonula occludens-1 in MWF rats. *J Am Soc Nephrol* 11:477–489, 2000

39. Laemmli UK: Cleavage of structural proteins during the assembly of the head of bacteriophage T4. *Nature* 227:680–685, 1970

40. Kawachi H, Koike H, Kurihara H, et al: Cloning of rat homologue of podocin: Expression in proteinuric states and in developing glomeruli. *J Am Soc Nephrol* 14:46–56, 2003

41. Kawamura A Jr.: Preparation of labeled antibody and staining method, in *Fluorescence Antibody Techniques and Their Applications* (2nd ed.), edited by Kawamura A Jr., Tokyo, University of Tokyo Press, 1977, pp 77–79

42. Benigni A, Tomasoni S, Gagliardini E, et al: Blocking angiotensin II synthesis/activity preserves glomerular nephrin in rats with severe nephrosis. *J Am Soc Nephrol* 12:941–948, 2001

43. Kerjaschki D, Sharkey DJ, Farquhar MG: Identification and characterization of podocalyxin—The major sialoprotein of the renal glomerular epithelial cell. *J Cell Biol* 98:1591–1596, 1984

44. Takeda T, McQuistan T, Orlando RA, Farquhar MG: Loss of glomerular foot processes is associated with uncoupling of podocalyxin from the actin cytoskeleton. *J Clin Invest* 108:289–301, 2001

45. Orlando RA, Takeda T, Zak B, et al: The glomerular epithelial cell anti-adhesin podocalyxin associates with the actin cytoskeleton through interactions with ezrin. *J Am Soc Nephrol* 12:1589–1598, 2001

46. Ohashi T, Uchida K, Uchida S, et al: Intracellular mislocalization of mutant podocin and correction by chemical chaperones. *Histochem Cell Biol* 119:257–264, 2003

47. Yuan H, Takeuchi E, Salant DJ: Podocyte slit-diaphragm protein nephrin is linked to the actin cytoskeleton. *Am J Physiol Renal Physiol* 282:F585–F591, 2002

48. Patari A, Forsblom C, Havana M, et al: Nephrinuria in diabetic nephropathy of type 1 diabetes. *Diabetes* 52:2969–2974, 2003

49. Luimula P, Aaltonen P, Ahola H, et al: Alternatively spliced nephrin in experimental glomerular disease of the rat. *Pediatr Res* 48:759–762, 2000

50. Aaltonen P, Luimula P, Astrom E, et al: Changes in the expression of nephrin gene and protein in experimental diabetic nephropathy. *Lab Invest* 81:1185–1190, 2001

51. Simons M, Schwarz K, Kriz W, et al: Involvement of lipid rafts in nephrin phosphorylation and organization of the glomerular slit diaphragm. *Am J Pathol* 159:1069–1077, 2001

52. Debiec H, Guigonis V, Mougenot B, et al: Antenatal membranous glomerulonephritis due to anti-neutral endopeptidase antibodies. *N Engl J Med* 346:2053–2060, 2002